Experimental Measurement and Theoretical Assessment of Fast Lanthanide Electronic Relaxation in Solution with Four Series of Isostructural Complexes

ARTICLE *in* THE JOURNAL OF PHYSICAL CHEMISTRY A · DECEMBER 2012

Impact Factor: 2.69 · DOI: 10.1021/jp311273x · Source: PubMed

5 AUTHORS, INCLUDING:

Alexander Max Funk
University of Texas Southwestern Medical Cen…
7 PUBLICATIONS **74** CITATIONS
SEE PROFILE

Peter Harvey
The University of Manchester
9 PUBLICATIONS **70** CITATIONS
SEE PROFILE

THE JOURNAL OF PHYSICAL CHEMISTRY A

Article

pubs.acs.org/JPCA

Experimental Measurement and Theoretical Assessment of Fast Lanthanide Electronic Relaxation in Solution with Four Series of Isostructural Complexes

Alexander M. Funk,[†] Pascal H. Fries,*[,‡] Peter Harvey,[†] Alan M. Kenwright,[†] and David Parker*[,†]

[†]Department of Chemistry, Durham University, South Road, Durham DH1 3LE, U.K.

[‡]CEA, INAC, Service de Chimie Inorganique et Biologique (UMR_E3 CEA UJF), 38054 Grenoble, France

Supporting Information

ABSTRACT: The rates of longitudinal relaxation for ligand nuclei in four isostructural series of lanthanide(III) complexes have been measured by solution state NMR at 295 K at five magnetic fields in the range 4.7−16.5 T. The electronic relaxation time T_{1e} is a function of both the lanthanide ion and the local ligand field. It needs to be considered when relaxation probes for magnetic resonance applications are devised because it affects the nuclear relaxation, especially over the field range 0.5 to 4.7 T. Analysis of the data, based on Bloch−Redfield−Wangsness theory describing the paramagnetic enhancement of the nuclear relaxation rate has allowed reliable estimates of electronic relaxation times, T_{1e}, to be obtained using global minimization methods. Values were found in the range 0.10−0.63 ps, consistent with fluctuations in the transient ligand field induced by solvent collision. A refined theoretical model for lanthanide electronic relaxation beyond the Redfield approximation is introduced, which accounts for the magnitude of the ligand field coefficients of order 2, 4, and 6 and their relative contributions to the rate $1/T_{1e}$. Despite the considerable variation of these contributions with the nature of the lanthanide ion and its fluctuating ligand field, the theory explains the modest change of measured T_{1e} values and their remarkable statistical ordering across the lanthanide series. Both experiment and theory indicate that complexes of terbium and dysprosium should most efficiently promote paramagnetic enhancement of the rate of nuclear relaxation.

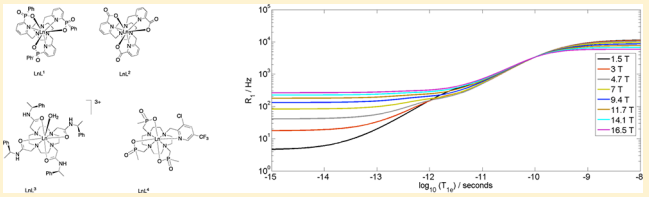

1. INTRODUCTION

The lanthanide ions of the second half of the f-block series combine very fast rates of electronic relaxation with high paramagnetic susceptibility. The fast rates of electronic relaxation allow observation of the resonances of ligand nuclei in their coordination complexes, aiding interpretation of complex geometry by analyzing the induced paramagnetic dipolar shifts.[1] In addition, intermolecular interactions of the complexes with solvent and closely diffusing or noncovalently bound molecules can be probed.[2−4] The high paramagnetic susceptibility of the ions promotes fast longitudinal and transverse relaxation of proximate nuclear spins.[5−7] Because of their steep dependence (r^{-6}) on the electron−nuclear distance, the intramolecular relaxation rates due to the dipolar coupling can be very fast at short distances. In the case of transverse relaxation rate, line-broadening may become severe and inhibit spectroscopic observation.

A. Electronic Relaxation from Nuclear Relaxation. The analysis of intramolecular nuclear relaxation rate data is most commonly addressed using Bloch−Redfield−Wangsness theory,[6] in which paramagnetic relaxation arises from rotational and conformational modulation of the electron−nuclear dipolar interaction, eqs 1 and 2.

$$R_1 = \frac{2}{15}\left(\frac{\mu_0}{4\pi}\right)^2 \frac{\gamma_N^{\,2} g_{Ln}^{\,2} \mu_B^{\,2} J(J+1)}{r^6} \times \left[3\frac{T_{1e}}{1+\omega_N^{\,2}T_{1e}^{\,2}} + 7\frac{T_{1e}}{1+\omega_e^{\,2}T_{1e}^{\,2}}\right] + \frac{2}{5}\left(\frac{\mu_0}{4\pi}\right)^2 \frac{\omega_N^{\,2}\mu_{eff}^{\,4}}{(3k_BT)^2 r^6}\left[3\frac{\tau_r}{1+\omega_N^{\,2}\tau_r^{\,2}}\right] \quad (1)$$

$$R_2 = \frac{2}{15}\left(\frac{\mu_0}{4\pi}\right)^2 \frac{\gamma_N^{\,2} g_{Ln}^{\,2} \mu_B^{\,2} J(J+1)}{r^6} \times \left[2T_{1e} + \frac{3}{2}\frac{T_{1e}}{1+\omega_N^{\,2}T_{1e}^{\,2}} + \frac{13}{2}\frac{T_{1e}}{1+\omega_e^{\,2}T_{1e}^{\,2}}\right] + \frac{2}{5}\left(\frac{\mu_0}{4\pi}\right)^2 \frac{\omega_N^{\,2}\mu_{eff}^{\,4}}{(3k_BT)^2 r^6}\left[2\tau_r + \frac{3}{2}\frac{\tau_r}{1+\omega_N^{\,2}\tau_r^{\,2}}\right] \quad (2)$$

where μ_0 is vacuum permeability, γ_N is the magnetogyric ratio of the nucleus, g_{Ln}, often loosely denoted by g_J, is the Landé factor of the fundamental multiplet J of the free Ln^{3+} ion, μ_B is the

Received: November 14, 2012
Revised: December 20, 2012
Published: December 21, 2012

Bohr magneton (BM), r is the electron−nuclear distance, τ_r is the rotational correlation time, ω_N is the nuclear Larmor frequency, $\omega_e = (g_{Ln}\mu_B/\hbar)B_0$ is the electron Larmor frequency, μ_{eff}^2 is the square of the effective magnetic moment of the coordinated Ln^{3+} ion used in the paramagnetic susceptibility theory,[8] T is the absolute temperature, k_B is the Boltzmann constant, and T_{1e} is the longitudinal relaxation time of the electron spin. Note that μ_{eff}^2 can often be accurately approximated as $\mu_{eff}^2 = g_J^2\mu_B^2\langle \mathbf{J}^2\rangle$, where $\langle \mathbf{J}^2\rangle \cong J(J+1)$ is the square of the electron angular momentum averaged over the thermally populated electronic energy levels. Because $T_{1e} \ll \tau_r$ for the studied Ln^{3+} ions, the usual correlation time $\tau_{r+e} = (\tau_r^{-1} + T_{1e}^{-1})^{-1} \cong T_{1e}$ is replaced by T_{1e} in the first terms in eqs 1 and 2. These terms arise from stochastic modulation of the electron−nuclear dipolar interaction by molecular rotation and random jumps of the electron magnetization. They become equal at $B_0 = 0$. The second terms are independent of the rate of electronic relaxation and can be ascribed to rotational modulation of the dipolar interaction of the nucleus with the average magnetic dipole moment induced by the applied magnetic field: this is often termed Curie relaxation.[6b] The second terms are also equal at vanishing field. Owing to the dependence of R_1 on μ_{eff}^4 in the Curie term, the second parts of eqs 1 and 2 become increasingly important at higher magnetic fields for the ions with large values of μ_{eff} (Table 1).

Table 1. Ground State J Values and Experimental Magnetic Moments$^+$ (BM) for the Fast Relaxing Ln^{3+} Ions

	Tb	Dy	Ho	Er	Tm	Yb
J	12/2	15/2	16/2	15/2	12/2	7/2
μ_{eff}/BM	9.8	10.3	10.4	9.4	7.6	4.3

Longitudinal relaxation rates, R_1, can be measured precisely, and by recording them for several ligand nuclei at a variety of magnetic fields, electron−nuclear distances, r, rotational correlation times, τ_r, and electronic relaxation times, T_{1e}, can either be estimated directly or be estimated using global minimization methods. This multiparameter approach has been used to estimate internuclear distances[5] and is applied here to assess values of T_{1e}. Related methods have been reported using ^{1}H NMR relaxation rate data for ligand resonances in $[Ln.DOTA(H_2O)]^-$ (Ln = Tb, Dy, Ho)[9] and $[Ln.DOTP]^{5-}$ (Ln = Tb, Dy, Ho, Er, Tm, Yb).[10] In the former case T_{1e} values were in the range 0.14−0.30 ps and fell in the order Tb > Dy > Ho; in the latter case, values were about a factor of 2 greater. Others have analyzed the variation of R_1 for dissolved lanthanide aqua ions or coordination complexes in water, examining the field and temperature dependence of the water proton relaxation rate.[8,11,12] In each case, values of T_{1e} were noted to be more or less independent of applied magnetic field and only slightly decreased with increasing temperature.

A physical model, to allow quantitative interpretation of T_{1e} data, has been promulgated recently.[13] It suggests that fluctuations in the transient (T) ligand field arising from solvent collisions lie at the origin of electronic relaxation in solution. Collisions of the complex with the solvent occur at a rate of 10^{13} s^{-1}, thereby setting a lower limit 10^{-13} s to T_{1e}. The model suggests that T_{1e} values should scale with $|J|$ and increases in the transient ligand field were calculated to lead to reductions in T_{1e}. However, the variation of T_{1e} with the nature of the Ln^{3+} ion, the symmetry, specific tensorial form, and the fluctuation rate of its transient ligand field, or the presence of a static (S) ligand field merit further investigation. Indeed, the coefficients $B_{T,q}^k$ of the transient ligand field were only roughly estimated from their static counterparts $B_{S,q}^k$, the determinations of which from optical emission spectra have revealed differences of an order of magnitude, in various site symmetries, with values of up to around 1000 cm^{-1}.[14,15] In view of the absence of an independent experimental method for assessing the value of the transient ligand field, the existence of a significant correlation between its coefficients $B_{T,q}^k$ and their static counterparts $B_{S,q}^k$ would be particularly useful. A full analysis of optical emission spectra, in principle, allows all the $B_{S,q}^k$ parameters to be assessed and this work should in future be considered, once it has been undertaken.

With this background in mind we have set out to examine the variation of T_{1e} in aqueous solution in four series of isostructural Ln(III) complexes. The aim was to correlate T_{1e} with the ligand field in these systems, as well as offering a more complete set of data to test the limits of the recent theoretical analysis.

B. Relevance to Magnetic Resonance Probe Design and Selection of Lanthanide Complexes. The set of lanthanide complexes studied is shown in Chart 1. In each case, an isostructural series has been defined for the Ln(III) ions selected. Thus, the pair of neutral complexes based on triazacyclononane involve tricapped trigonal prismatic coordination; $[Ln.L^1]$[16] and $[Ln.L^2]$[17] possess C_3 symmetry and differ only in the anionic donor group (phenylphosphinate vs carboxylate). Crystal structures of the whole Ln series of complexes with L^1 have been determined.[16] The cationic tetraamide complexes, $[Ln.L^3]$, involve a monocapped square antiprismatic coordination geometry. Crystal structure analyses have also been undertaken across the whole series[18,19] and reveal that each complex possesses C_4 symmetry. The fourth set of complexes, $[Ln.L^4]$, involves a monopyridyl-triphosphinate ligand and each complex adopts a preferred twisted square antiprismatic (octadentate) coordination geometry, similar to that defined for related monoamide triphosphinate systems.[20] The presence of the ^{31}P nucleus in L^1 and the ^{19}F label in L^4, allows analysis of multinuclear relaxation rate data, (^{1}H, ^{19}F, ^{31}P NMR).

Chart 1. Structures of the Isostructural Lanthanide Complex Series $[Ln.L^{1-4}]$ Analyzed

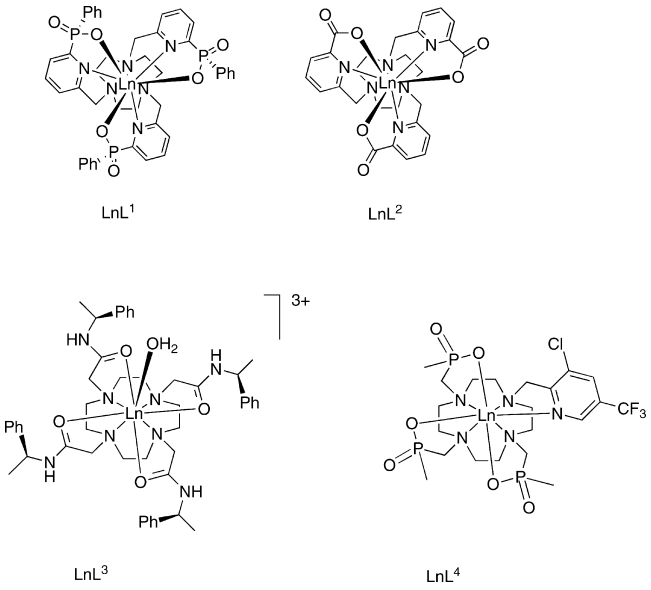

dx.doi.org/10.1021/jp311273x | J. Phys. Chem. A 2013, 117, 905−917

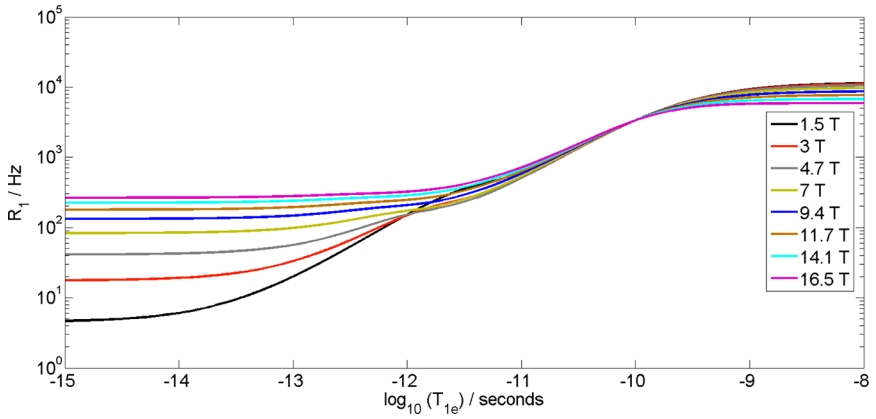

Figure 1. Simulation of the dependence of the ^{19}F relaxation rate, R_1, on electronic relaxation rate at different magnetic field strengths (μ_{eff} = 10 μ_B, r = 6 Å, τ_r = 250 ps, at 295 K).

Table 2. Measured ^{31}P Relaxation Rates, R_1[a] (Hz), of [Ln.L^1] and Corresponding Calculated Values for the Internuclear Ln−P Distance, r (Å), the Rotational Correlation Time, τ_r (ps), and the Electronic Relaxation Time, T_{1e} (ps) at 295 K

		R_1/Hz					fitting values		
Ln^{3+}	δ_P/ppm	4.7 T	9.4 T	11.7 T	14.1 T	16.5 T	τ_r/ps	T_{1e}/ps	r/Å
Tb	−38.1	242	603	824	1071	1322	356	0.30	3.9
Dy	−23.8	332	876	1213	1619	1978	352	0.25	3.8
Ho	−8.4	242	603	824	1071	1322	304	0.17	3.8
Er	35.8	248	533	745	963	1202	288	0.36	3.8
Tm	54.6	64	194	271	358	463	291	0.09	3.9
Yb	20.7	11	24	34	42	54	278	0.08	3.8
	av						293		3.9

[a]The experimental error was below 10% in all measurements.

A strong motivation of this study is the development of magnetic resonance relaxation probes for the chemical and biological sciences.[5] Using eq 1, the impact of T_{1e} on R_1 values can be calculated (Figure 1), taking reasonable estimated values for the key variable parameters in a putative low MW probe complex (τ_r = 250 ps, μ_{eff} = 10 μ_B (Table 1).

What is immediately apparent from Figure 1 is the striking influence T_{1e} has in determining R_1 over the field range 1.5−7 T. This is the range of most modern MR imaging instruments; current clinical MRI instruments operate at 1.5 or 3 T. Similar simulations have been undertaken for a ^1H MR probe (Supporting Information) and the variations of R_2 (eq 2) echo those shown for R_1, to a first approximation. Thus, an increase in T_{1e} from 0.22 to 0.44 ps causes an 86% increase in R_1 at 1.5 T, 62% at 3 T, and 22% at 7 T.

For a putative ^{31}P MR probe, a reasonable assumption is that the ligand would incorporate a P(V) oxy-anion donor to coordinate the paramagnetic ion. In this case, the Ln−P distance r is about 3.6 Å.[16] If T_{1e} is 0.11 ps, R_1 is calculated to be 86 Hz at 1.5 T and 140 Hz at 3 T, rising to 154 and 206 Hz, respectively, when T_{1e} doubles in magnitude (Supporting Information). Evidently, values of T_{1e} need to be considered in the design of an MR relaxation probe, so that a better understanding is required of the relationship between ligand/complex structure, lanthanide ion selection and target values of R_1/R_2.[5a,19,20]

2. EXPERIMENTAL SECTION

A. NMR Data Acquisition. ^1H, ^{19}F and ^{31}P NMR relaxation rates were obtained at 295 K on Varian spectrometers operating at 4.7, 9.4, 11.7, 14.1, 16.5 T, specifically a Mercury 200 spectrometer (^1H at 200.057 MHz, ^{19}F at 188.242 MHz, ^{31}P at 80.985 MHz), a Mercury 400 spectrometer (^1H at 399.97 MHz, ^{19}F at 376.331 MHz, ^{31}P at 161.91 MHz), a Varian Inova-500 spectrometer (^1H at 499.78 MHz, ^{19}F at 470.322 MHz, ^{31}P at 125.67 MHz), a Varian VNMRS-600 spectrometer (^1H at 599.944 MHz, ^{19}F at 564.511 MHz, ^{31}P at 242.862 MHz) and a Varian VNMRS-700 spectrometer (^1H at 699.73 MHz, ^{19}F at 658.658 MHz, ^{31}P at 283.365 MHz). Commercially available deuterated solvents were used.

The operating temperature of the spectrometers was measured with the aid of an internal calibration solution of ethylene glycol. The operating temperature of each spectrometer was measured before each set of measurements of relaxation data, using the calibration sample.

Longitudinal relaxation data were measured using the inversion−recovery technique. For ^{19}F and ^{31}P the relaxation data were measured without proton decoupling. For ^{31}P analyses, the chemical shifts are reported relative to 85% phosphoric acid. For ^{19}F analyses, the chemical shifts are reported relative to fluorotrichloromethane.

The recorded free induction decays were processed using backward linear prediction, optimal exponential weighting, zero-filling, Fourier transform, phasing and baseline correction (by polynomial fitting). The signals were integrated by Lorentzian line fitting.

The ^{31}P rates of the series [Ln.L^1] and the individual fitting values can be found in Table 2. For the analysis of the ligand ^1H resonances of each lanthanide complex, typically six ^1H resonances were used to calculate individual internuclear distances, rotational correlation and electronic relaxation times. These values were then averaged to produce the overall fitted values (see Supporting Information Table 1 for further data and

dx.doi.org/10.1021/jp311273x | J. Phys. Chem. A 2013, 117, 905−917

information). Additional tables for the remaining lanthanide series' can be found in the Supporting Information (Tables 2–4) or are available from the authors on request.

B. Data and Error Analysis. Relaxation data was fitted by using a modified Matlab algorithm, originally written by Dr. Ilya Kuprov of Southampton University. The rate data were analyzed using an algorithm, based on internal Levenberg–Marquardt minimization of the nonlinear least-squares error function; results were analyzed iteratively, allowing values of T_{1e}, τ_r, μ_{eff}, and r to minimize for all data sets (global fitting). In addition, minimizations were also computed using fixed values of μ_{eff}[7] and, separately, using the internuclear distances, r, derived from the published X-ray structural analyses.[16−18] Some parameters were used globally for every Ln(III) complex in the series and others were used for each complex individually. The rotational correlation time, τ_r, was considered not to vary across one series of complexes. An estimate for τ_r was made using the Stokes–Einstein law. Following a DFT calculation, the hydrodynamic radius, r, was also estimated by inspecting the published X-ray data;[15,16] in each case a reasonable agreement was found (±0.2 Å).

The magnetic moments for each lanthanide ion were taken from the literature[7] or were allowed to vary in the minimization. Each relaxation measurement was repeated at least three times and the mean value recorded. The number of transients used in the measurements was determined by the signal-to-noise ratio and therefore primarily by the concentration of the complex solution. In each case, the signal was fully recovered during the inversion–recovery sequence.

An experiment was performed to calculate the error associated with the temperature variance of the spectrometers, as the measured rates are particularly T sensitive. The relaxation rate of [Tm.L^1] was measured at five different temperatures (295–303 K in 2 K steps) at 16.5 T. At each measurement, the temperature was also determined by using the temperature calibration sample (^{1}H NMR: ethylene glycol). In the Curie term of the Solomon–Morgan–Bloembergen equations (eq 1 above), the temperature dependence of the relaxation rate, R_1, varies as $1/T^2$. The variation of R_1 with T arising from this dependence becomes more significant at higher magnetic fields. The temperature dependence of the rotational correlation time τ_r is also important in this context. It is directly proportional to solvent viscosity, and varies as $e^{\Delta E/RT}$. Given an error in T measurement of 0.5 K, the error in the R_1 measurement was estimated to be less than 1.5% (Table 3) and was primarily associated with the T^{-2} dependence

Table 3. ^{31}P NMR Relaxation Rates (Hz) at a Range of Temperatures (K) for [Tm.L^1]^a

R_1	T	$1/T^2 \times 10^{-3}$
463	295	0.0115
446	296.8	0.0114
426	298.5	0.0112
413	300.6	0.0111
397	302.2	0.0109

^{a}Using ^{31}P NMR relaxation rate data for [Tm.L^1] (1 mM), measured at 16.5 T in CD_3OD.

of R_1. This error was assumed to be similar for each complex studied.

A complex error analysis was undertaken. The experimental errors of the measured relaxation rates were combined and used to perturb the relaxation rates for each complex at each field. These perturbed rates were used in a Monte Carlo error analysis to obtain the fitting error for the individual parameters (μ_{eff}, r, τ_r, and T_{1e}) calculated in the minimization process.

3. RESULTS

A. Experimental Results. The rates of longitudinal relaxation, R_1, of ligand resonances (^{1}H, ^{19}F, ^{31}P) in the complexes [Ln.L$^{1-4}$] were measured at 295 K. Solutions were made in D_2O with a 1 mM complex concentration, except for [Ln.L^1], which is sparingly soluble in water, for which CD_3OD was the solvent. The different solvent viscosity values have a direct effect on the rotational correlation time, τ_r, and therefore show reduced relaxation rates, R_1, for [Ln.L^1] when compared to [Ln.L^2]. Figure 2 shows the fitting of the eq 1 using the data points shown in Table 2.

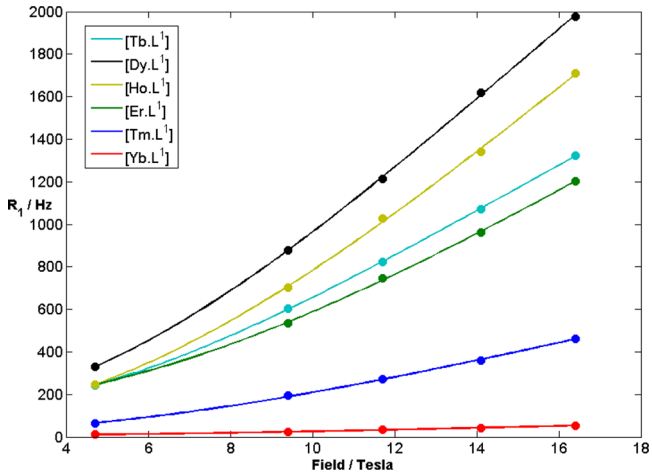

Figure 2. Variation of ^{31}P R_1 with magnetic field for [Ln.L^1] (295 K, CD_3OD) showing the fit (line) to the experimental data, using a fixed value of μ_{eff} in the minimization.

Values for the fitted parameters T_{1e} and τ_r, obtained by the fitting procedure with constrained μ_{eff} values are reported in Table 4. Further figures that depict the fitting for each complex series can be found in the Supporting Information. With [Ln.L^1], ^{1}H and ^{31}P rate data analyses showed good agreement with values of T_{1e} consistent within one standard deviation.

The values of T_{1e} are smallest for the complexes of L^1 and L^2 that adopt a trigonal trigonal prismatic geometry and are largest for the complexes of L^3 and L^4 that take up a twisted or monocapped square antiprismatic geometry. Values of τ_r followed the sequence [Ln.L^3] > [Ln.L^4] > [Ln.L^1] > [Ln.L^2], in accord with the variation in molecular volume estimated by DFT calculations from the Connolly surface. The higher value of τ_r was found by analysis of ^{31}P rate data for [Ln.L^1], compared to that estimated from ^{1}H NMR data and probably reflects the difference in the degree of motional coupling. The ^{31}P nuclei lie close to the barycenter of the complex and have few degrees of freedom; their motion is efficiently coupled to the overall molecular rotation. In contrast, the motion of more remote ligand nuclei is not likely to be so well coupled, and the apparent τ_r value is reduced. Data were also analyzed using fixed values of r (Table 5), allowing T_{1e} and μ_{eff} to minimize.

The estimated values of T_{1e} were within one standard deviation of those assessed by fixing μ_{eff}, and the "best fit" values of μ_{eff} show good correspondence with those measured experimentally.[7]

dx.doi.org/10.1021/jp311273x | J. Phys. Chem. A 2013, 117, 905–917

Table 4. Calculated Values of T_{1e} [a,b,c] (ps) and τ_r (ps) for the Given Isostructural Series Analysing ^{1}H and ^{19}F NMR R_1 Data for Each Complex Individually, with Errors in Parentheses

	L^1 [d]	L^2	L^3	L^4 [e]
Tb	0.27 (0.02)	0.24 (0.03)	0.54 (0.06)	0.50 (0.03)
Dy	0.30 (0.04)	0.24 (0.02)	0.43 (0.03)	0.46 (0.03)
Ho	0.18 (0.07)	0.15 (0.02)	0.34 (0.01)	0.41 (0.03)
Er	0.31 (0.06)	n.d.	0.31 (0.09)	0.63 (0.02)
Tm	0.09 (0.02)	0.08 (0.02)	0.20 (0.02)	0.26 (0.02)
Yb	0.11 (0.03)	0.07 (0.03)	0.17 (0.03)	0.37 (0.02)
τ_r/ps	190 (17)	138 (8)	353 (30)	241 (12)

[a]All T_{1e} values are estimated on the basis of the average of rate data for at least five common ^{1}H resonances measured. [b]Data for complexes of L^1 were obtained in CD_3OD, whereas other series were measured in D_2O (vide infra for any solvent dependence). [c]The effective magnetic moment, μ_{eff}, was fixed in these calculations. The values used were Tb (9.8), Dy (10.3), Ho (10.4), Er (9.4), Tm (7.6), and Yb (4.3) BM. [d]^{31}P longitudinal relaxation rate measurements were also undertaken and led to estimates of T_{1e} (ps) as follows: Tb, 0.30(01); Dy, 0.25(03); Ho, 0.17(01); Er, 0.36(01); Tm, 0.09(02); Yb, 0.08(02); τ_r = 311(5) ps. [e]For L^{1-3}, ^{1}H relaxation data were used and for L^4 ^{19}F data were used.

B. Control Experiments and Calculations. The data analyzed by fitting the rate data with fixed values of μ_{eff} (Table 4) also generate internuclear distances, r, between the resonances observed and the coordinated lanthanide ion. For the complexes of L^1 and L^3 for which full X-ray structural data has been reported, this allows estimated and experimental values to be compared (Table 6). Although there are some discrepancies, the agreement is quite good particularly for complexes of L^3. Geometric parameters for a solution state structure do not necessarily correspond to those observed in a frozen lattice at 120 K.

For the $[Ln.L^1]$ series of complexes the dependence of the relaxation rate, R_1, with distance was assessed for five different systems at 4.7 T (Figure 3 and Supporting Information for data). The values of r used in this analysis were those reported in the X-ray analyses. A plot of R_1 vs r^{-6} is linear in each case, confirming the ligand NMR assignments unequivocally. At the very least, these "internal checks" give confidence in the values of T_{1e} estimated by the two different minimization methods used.

A further independent "test" of the validity of this approach is to examine the variation of estimated τ_r values, arising from modulation of solvent viscosity. In a classical Stokes−Einstein approximation, τ_r is directly proportional to solvent viscosity. Accordingly, relaxation rates (Table 7) were measured for $[Ln.L^3]^{3+}$ in D_2O, CD_3OD, and CD_3CN at five fields. These are solvents in which the viscosity (298 K) falls from 1.13 (D_2O) to 0.60 (CD_3OD) and 0.36 (CD_3CN).[21]

Table 6. Estimated[a] and Experimental (X-ray, Solid State[b] ±0.02 Å) Mean Values of the Internuclear Distance, r (Å), with Errors in Parentheses

	L^1		L^3	
ligand proton[c]	est	exp	est	exp
H_{ax}	4.34 (0.14)	4.12	3.90 (0.01)	3.73
$H_{ax'}$	3.97 (0.001)	3.45	3.57 (0.01)	3.69
H_{eq}	4.54 (0.03)	4.30	4.48 (0.11)	4.37
$H_{eq'}$	4.55 (0.03)	4.35	4.48 (0.10)	4.37
pyCHN/CHCO[c]	4.45 (0.04)	4.35	4.40 (0.19)	4.26
pyCHN/CHCO	3.48 (0.001)	3.50	3.75 (0.003)	3.67

[a]Estimated using a fixed μ_{eff} (see above). [b]Taken from X-ray crystallographic studies.[15,16] [c]H_{ax} and H_{eq} refer to the axial and equatorial protons in the five-membered chelate ring defined by $NCH_2CH_2NL_n$; pyCHN refers to the pyridyl methylene proton in L^1 and CHCO refers to one of the NCH_2CO protons in L^3.

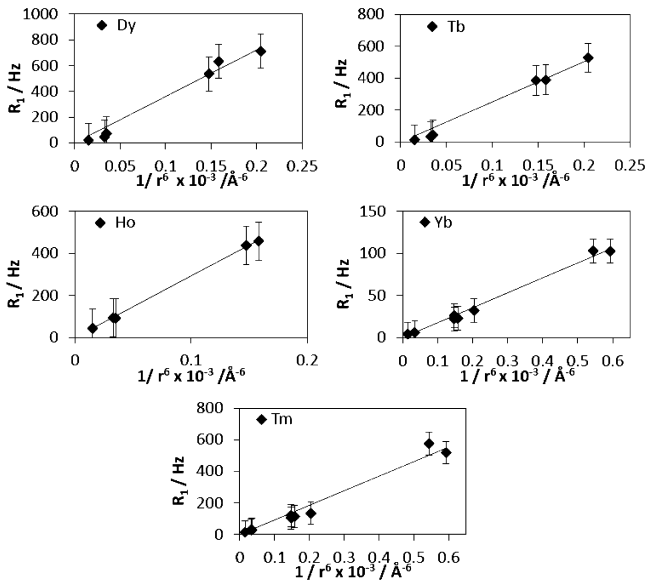

Figure 3. Dependence of relaxation rate, R_1, on the lanthanide to proton internuclear distance, r^{-6}, for the $[LnL^1]$ series (4.7 T, 295 K). Values of r were derived from X-ray crystallographic studies. The intercept in each case theoretically gives the diamagnetic contribution to the measured R_1 value, which is of the order of 1 Hz.

The values of r, τ_r, and T_{1e} were allowed to vary, holding values of μ_{eff} constant, and in each case the values of r corresponded well to those determined by X-ray analysis. The electronic relaxation times showed no dependence on solvent viscosity, and the values of τ_r estimated were 353(30) ps for D_2O, 253(18) ps for CD_3OD,

Table 5. Calculated Values of T_{1e}[a] (ps) Obtained through Global Fitting Procedures Analysing R_1 Data for Common ^{1}H Resonances within Each Isostructural Series,[b] with Fitting Errors in Parentheses

	L^1		L^2		L^3	
	T_{1e}	μ_{eff}/BM	T_{1e}	μ_{eff} /BM	T_{1e}	μ_{eff} /BM
Tb	0.21 (0.04)	9.40 (0.03)	0.29 (0.01)	9.62 (0.01)	0.57 (0.003)	9.23 (0.01)
Dy	0.32 (0.03)	10.21 (0.03)	0.29 (0.01)	10.38 (0.01)	0.42 (0.003)	10.30 (0.01)
Ho	0.11 (0.02)	10.22 (0.01)	0.18 (0.01)	10.54 (0.002)	0.31 (0.01)	9.91 (0.01)
Er	0.26 (0.03)	9.05 (0.02)				
Tm	0.09 (0.04)	7.66 (0.03)	0.08 (0.02)	7.49 (0.002)	0.28 (0.01)	7.57 (0.01)
Yb	0.12 (0.06)	4.35 (0.02)	0.07 (0.03)	4.34 (0.03)	0.21 (0.02)	4.34 (0.03)

[a]All T_{1e} values are based on the analysis of data for at least five common ^{1}H resonances for each series. [b]The internuclear distance, r, was fixed in these calculations.

dx.doi.org/10.1021/jp311273x | J. Phys. Chem. A 2013, 117, 905−917

Table 7. Effects of Different Solvents on the Estimated Electronic, T_{1e} and Rotational Correlation Time, τ_r (ps), in the [LnL^3] Series, with Errors in Parentheses

	D_2O		CD_3OD[a]	
	T_{1e}	τ_r	T_{1e}	τ_r
Tb	0.54 (0.06)	341	0.50 (0.05)	257
Dy	0.43 (0.03)	330	0.41 (0.04)	249
Ho	0.34 (0.01)	360	0.22 (0.06)	257
Tm	0.20 (0.02)	381	0.19 (0.04)	266
Yb	0.17 (0.03)	343	0.16 (0.03)	238
Mean τ_r		353 (30)		253 (18)

[a]Values for Tb and Yb were also measured in CD_3CN and gave a mean τ_r value of 162(12) ps, with T_{1e} estimated to be 0.52(05) ps for the Tb complex and 0.15(03) ps for the Yb analogue.

and 162(12) ps for CD_3CN. These values are in reasonable agreement with the variation of τ_r with viscosity.

4. DISCUSSION

A self-consistent analysis of the field dependence of NMR relaxation rate data in four well-defined series of Ln(III) complexes has allowed values of T_{1e} to be determined, with reasonable accuracy and confidence. The values of T_{1e} across each series fall into groups, with [Tb, Dy, Er] > Ho > [Tm > Yb]. This sequence does not simply reflect the degeneracy of J states (Table 1), with the values for Ho (J = 16/2) being surprisingly low in each system. Earlier, Williams using low field measurments had noted[11] that in the isostructural, C_3-symmetric series of [Ln(DPA)$_3$] complexes, values of T_{1e} were as follows: Tb, 0.29 ps; Dy, 0.45 ps; Ho, 0.17 ps; Er, 0.32 ps; Tm, 0.16 ps; Yb, 0.10 ps. Similarly, Aime had shown for [Ln.DOTA(H_2O)]$^-$ systems that T_{1e} values were 0.30 ps for Tb, 0.25 ps for Dy and 0.15 ps for Ho. Thus, the lower values for Ho have clear precedent and are reaffirmed here. This finding has significance in the selection of a lanthanide ion when a paramagnetic probe is devised. Although complexes of Ho have the largest value of μ_{eff} (10.4 μ_B), those of erbium, terbium, or dysprosium are preferred at lower field, where the impact of a low T_{1e} value is most important in determining R_1 (and R_2). This is emphasized in a model calculation (Table 8), using a ^{1}H probe nucleus in hypothetical

Table 8. Calculated ^{1}H Relaxation Rates, R_1 (Hz), at Various Magnetic Fields (T) for Ho(III) and Er(III) at the Given Internuclear Distances (τ_r = 250 ps, 295 K)

		field/T				
		1.5	3	4.7	7	9.4
r = 5 Å	Ho[a]	120	171	261	419	601
	Er[b]	155	187	244	345	459
r = 6 Å	Ho	40	57	87	140	201
	Er	52	63	82	115	154
r = 7 Å	Ho	16	23	35	56	80
	Er	21	25	33	46	61

[a]Ho(III) values are calculated with μ_{eff} = 10.4 μ_B and T_{1e} = 0.18 ps. [b]Er(III) values are calculated with μ_{eff} = 9.4 μ_B and T_{1e} = 0.31 ps.

complexes where the spin label is 5, 6, or 7 Å from the Ln ion. Values of R_1 are higher at 1.5 or 3 T for Er, Tb, and Dy over the Ho analogue.

The physical model for electronic relaxation introduced recently by Fries and Belorizky highlights an inverse relationship between the transient ligand field induced by solvent collision and the size of T_{1e}.[13] The detailed analysis of static and transient ligand fields is complex. Rigorous determinations of the various static ligand field parameters $B^k_{S,q}$ that apply in the relevant local symmetry are only possible by analyzing optical emission spectra but are seldom undertaken.[14,15] For the [Ln.L$^{1-4}$] complexes, such an analysis has yet to be made. However, some information on $B^2_{S,0}$ is readily available, either directly by analysis of the splitting in the ΔJ = 1 multiplets for the Eu complex emission spectrum (splitting = $0.3B^2_{S,0}$)[22] or indirectly by a comparative analysis of NMR dipolar shifts.[23,24] For the europium complexes of L$^{1-4}$, solution emission spectra were analyzed (Table 9) and

Table 9. Second-Order Crystal Field Coefficients, $B^2_{S,0}$ (cm^{-1}), Devised from Analysis of Eu Emission Spectra in D_2O (295 K),[a] Errors in Parentheses Related to Spectral Resolution Limits

complex	$B_{S,0}{}^2$/cm^{-1}
[Eu.L^4]	−550 (40)
[Eu.L^3]	−470 (40)
[Eu.L^1]	+110 (40)
[Eu.L^2]	+75 (40)

[a]The sign of this coefficient is determined readily by the sense of the NMR dipolar pseudocontact shift in each case.[22]

the order of $B^2_{S,0}$ values was [Eu.L^4] > [Eu.L^3] > [Eu.L^1] > [Eu.L^2]. This order is the same as that observed in the T_{1e} values for the six Ln(III) ions in their complexes with L^1–L^4 (Tables 4 and 5).

This finding is inconsistent with a possible usage of the original relaxation model[13] in which the transient ligand field parameter $B^2_{T,0}$ would govern electronic relaxation and be strictly proportional to $B^2_{S,0}$, yielding a T_{1e} value inversely related to $|B^2_{S,0}|$. Because of the available information on $B^2_{S,0}$, it is particularly interesting to explore the effect of the second-order coefficients on the variation of T_{1e} across a given isostructural series. In a first approach,[13] it was assumed that electronic relaxation stems from a single tensorial term of the transient ligand field with constant norm. To go beyond this simplifying hypothesis, the effects of the various coefficients $B^k_{T,q}$ of the transient ligand field should be investigated together with the accompanying role of the static ligand field. Accordingly, the theoretical approach was revisited, taking these points of debate into account.

5. REVISED THEORETICAL ASSESSMENT OF ELECTRONIC RELAXATION

We set out to explain the general trend in T_{1e} along the series of complexes of heavy paramagnetic Ln^{3+} ions from Tb^{3+} to Yb^{3+}. The T_{1e} values measured here should be particularly reliable because they were derived from an intramolecular nuclear relaxation model with consistent control of the accuracy. The quality of the present data can be fully appreciated in comparison with the T_{1e} estimates in the aqua complexes obtained by different authors[8,11,12] from the relaxation rates of the protons on intermolecular probes such as water and $(CH_3)_4N^+$. The noticeable dispersion of the values reported by the different authors suggests questionable assumptions on the relative distribution and motion of these probes with respect to the Ln^{3+} ions. However, the sequences of values across the Ln^{3+} series are globally preserved. Then, the T_{1e} estimates obtained from intermolecular relaxation probes can be reasonably used from a statistical point of view, in the absence of safer data.

dx.doi.org/10.1021/jp311273x | J. Phys. Chem. A 2013, 117, 905−917

According to the published data of Aime et al.,[9] Ren and Sherry,[10] Williams et al.,[11] and those reported herein, the T_{le} values for several series of isostructural complexes range from about 0.1 to 0.6 ps. Statistically, across a given series, they seem to obey the sequence $T_{le}[Tb, Dy] \geq_{stat} T_{le}[Er] \geq_{stat} T_{le}[Ho] \geq_{stat} T_{le}[Tm] > T_{le}[Yb]$, where the symbol $\geq_{stat}$ means "statistically longer than". Indeed, the previous T_{le} order shows a few noticeable variations. For instance, $T_{le}[Er]$ is somewhat shorter than $T_{le}[Ho]$ in the EDTA, bis-DPA, DTPA, and present L^3 complexes, $T_{le}[Tm]$ is oddly long in the aqua, DTPA, and DOTP complexes. However, $T_{le}[Yb]$ always has the shortest value $\cong$0.1 ps with $T_{le}[Tm]$ often just slightly longer. Besides, as already noted, $T_{le}[Ho]$ can be significantly shorter than $T_{le}[Tb,Dy,Er]$.

The electronic relaxation of a complexed heavy Ln^{3+} ion in solution results from the random time-fluctuating Hamiltonians acting on its ground J multiplet and expressed in the laboratory (L) frame. The ligand field Hamiltonian[25−28] H_{lig} is by far the main cause of relaxation because of its dominant size. In a molecular (M) frame rigidly bound to the mean geometry of the complex, $H_{lig}(t)$ is the sum of its time-averaged value $H_{lig,S}$, named static (S) ligand field because of its time independence in (M) and of a residual fluctuating transient (T) ligand field Hamiltonian $H_{lig,T}(t) = H_{lig}(t) - H_{lig,S}$.[13] In the (L) frame, the fluctuations of the total Hamiltonian H_{lig} stems from those of $H_{lig,S}$ and $H_{lig,T}(t)$, due to the Brownian rotation of the complex and to its distortions and/or vibrations, respectively.

The general theory of electronic relaxation of a paramagnetic Ln^{3+} ion, including Gd^{3+}, rests on the time evolution of its density matrix.[29,30] In the context of the paramagnetic enhancement of nuclear relaxation rates and electron paramagnetic resonance (EPR), the effects of electronic relaxation can be simply described by quantum time correlation functions (TCFs), involving components of the angular momentum **J** of the ground multiplet.[31−34] The complexes of Gd^{3+} have attracted much attention as potential contrast agents in MR imaging because this ion has the largest possible electronic spin **S** = 7/2 with a particularly slow electronic relaxation, causing a strong acceleration of the relaxation of the neighboring nuclei.[35] In this context, many experimental and theoretical studies have led to a reasonable understanding of the electronic relaxation of Gd^{3+}, which can be ascribed to the fluctuations of its static and transient zero field splitting (ZFS) Hamiltonians.[36−40] A clear description is facilitated because these Hamiltonians can generally be approximated by simple second-order tensorial terms of small magnitudes (norms) < 1 cm^{-1}, giving rise to relaxation effects, the predicted variation of which with external field and/or temperature can be easily tested against experiment. In contrast, in the case of the other paramagnetic Ln^{3+} ions, tensorial terms of order 2, 4, and 6 and typical magnitudes $\geq$100 cm^{-1} contribute simultaneously and significantly to both the static and transient parts of their ligand field Hamiltonian, giving rise to very fast electronic relaxation with weak field and temperature variation.[13] Therefore, the investigation of the relaxation is still a challenge.

To disentangle the mechanisms at the origin of the electronic relaxation of the heavy Ln^{3+} from Tb^{3+} to Yb^{3+}, a two-step approach is proposed, starting from the following recent theoretical results.[13] Electronic relaxation is an incoherent process that can only be ascribed to fluctuating Hamiltonians with correlation times $\tau_c <\cong T_{le}$ where the symbol $<\cong$ means "shorter than or roughly equal to" and T_{le} is the experimental value in the range 0.1−0.6 ps. Thus, the fluctuations of $H_{lig,S}$ in (L) due to the tumbling of the complex of long rotational correlation time $\tau_r \geq 100$ ps cannot explain the fast observed electronic relaxation. In contrast, the bombardment of the complex by the solvent molecules at the rate of 10^{13} s^{-1} gives rise to the fluctuations of $H_{lig,T}$ of very short "vibrational" correlation time $\tau_v \cong 0.1$ ps, making it possible for the transient ligand field Hamiltonian to be at the origin of that electronic relaxation. Reasonable estimates of the magnitude (norm) $\|H_{lig,T}\|$ of $H_{lig,T}$ justify this working hypothesis. Moreover, because $\|H_{lig,T}\|\tau_v <\cong 1$, the approximate analytical theory of relaxation due to Redfield holds and gives the $1/T_{le}$ value in eq 6, which is simply proportional to the square $\|H_{lig,T}\|^2$. Then, the various tensorial terms of order 2, 4, 6 in $H_{lig,T}$ contribute to $1/T_{le}$ in proportion to the squares of their own magnitudes according to eq 6.

In the first step of the theoretical approach, electronic relaxation is studied within the simplifying approximation of Redfield, which applies with reasonable accuracy to the sole transient ligand field $H_{lig,T}$. The contributions to $1/T_{le}$ of the various tensorial terms in $H_{lig,T}$ are examined across the Ln^{3+} series. In the absence of independent experimental determination of $H_{lig,T}$, we show how rough estimates of $H_{lig,T}$ can be inferred from $H_{lig,S}$. In the second theoretical step, a Monte Carlo method is used for simulating the fluctuations in the (L) frame of both $H_{lig,S}$ and $H_{lig,T}$. The shortening of T_{le} by $H_{lig,S}$ is computed and discussed. "Exact" relaxation results are obtained and compared with the experimental trend. Note that for the investigated complexes, the information on $H_{lig,S}$, if any, is only partial. Thus, the rationale of the T_{le} sequence will be sought among the overall properties and values of the ligand field Hamiltonians of 4f elements.[25−27]

A. Tensorial Form of the Ligand Field Hamiltonian and Redfield Approximation. To begin with, the ligand field Hamiltonian is expressed in a tensorial form that is suitable for interpreting the relaxation properties.[13] The static (S) and transient (T) ligand field Hamiltonians can be written as linear combinations of the components of normalized (nor) Racah spherical tensors t_q^k

$$H_{lig,X} = \sum_{k,q} B_{X,q}^{nor,k} t_q^k \qquad (X = S \text{ or } T) \tag{3}$$

where the operators t_q^k are defined in terms of 3j-symbols by

$$\langle JM'|t_q^k|JM\rangle = (-)^{J-M'}\sqrt{2k+1}\begin{pmatrix} J & k & J \\ -M' & q & M \end{pmatrix} \tag{4}$$

The energy parameters $B_{X,q}^{nor,k}$ are normalized crystal field coefficients. Let

$$\|H_{lig,X}\| = \sqrt{\sum_{k,q} |B_{X,q}^{nor,k}|^2} \tag{5}$$

be the norm of $H_{lig,X}$. The electronic relaxation rates $R_{le} \cong R_{2e}$ of the complexed Ln^{3+} ion are approximated by the Redfield longitudinal relaxation rate at zero field

$$R_{1e}^{Redfield} = 1/T_{1e}^{Redfield} = (2\pi c_{light}\|H_{lig,T}\|)^2 \frac{6\tau_v}{(2J+1)J(J+1)} \tag{6}$$

due to $H_{lig,T}$ (cm^{-1}) with vibrational correlation time $\tau_v = \tau_{v,2}$. Furthermore, $T_{1e}^{Redfield}$ and $R_{1e}^{Redfield}$ are lower and upper bounds of T_{le} and R_{le}, respectively.[13] The norm $\|H_{lig,T}\|$ is of similar magnitude as the norm $\|H_{lig,S}\|$ of the static ligand field, which is about 20−30% larger (ref 13, Table 1) than its total energy splitting Δ_S ranging between 100 and 500 cm^{-1}. Because the distortions and vibrations of the complex stem from its collisions

dx.doi.org/10.1021/jp311273x | J. Phys. Chem. A 2013, 117, 905−917

with the solvent molecules at the frequency 10^{13} s^{-1}, the vibrational correlation time is typically $\tau_v \cong 0.1$ ps. Then, for the intermediate magnitude $\|H_{lig,T}\| \cong 300$ cm^{-1}, the values of $T_{1e}^{Redfield}$ of the various complexed Ln^{3+} ions span the interval from 0.06 ps for Yb^{3+} to 0.6 ps for Ho^{3+}. This theoretical range is in overall agreement with that defined by the measured values. However, the statistical experimental order of the T_{le} values across the Ln^{3+} series is not reproduced by the Redfield approximation, as shown by the ratios $T_{1e}^{Redfield,Ln}/T_{1e}^{Redfield,Yb}$ proportional to $(2J + 1)J(J + 1)$ and reported in Table 10. For instance, the

Table 10. $T_{le}^{Redfield,Ln}/T_{le}^{Redfield,Yb}$ from Tb^{3+} to Yb^{3+}

Tb	Dy	Ho	Er	Tm	Yb
4.33	8.1	9.71	8.1	4.33	1

overall variation of the experimental ratios T_{1e}^{Ln}/T_{1e}^{Yb} is 2 times less than that of their Redfield counterparts and the measured T_{le} values for Ho^{3+} are not the longest ones!

Despite its defects, the Redfield relaxation rate $R_{1e}^{Redfield}$ due to $H_{lig,T}$ is a reasonable estimate of the experimental T_{le} so that it is worth investigating whether the T_{le} order is related to the relative contributions of the various ligand field terms $B_{T,q}^{nor,k}t_q^k$ to $R_{1e}^{Redfield}$. According to eqs 5 and 6, these contributions are simply given by $|B_{T,q}^{nor,k}|^2$. There is no independent determination of the parameters $B_{T,q}^{nor,k}$ so that they have to be inferred from their counterparts of the static ligand field $B_{S,q}^{nor,k}$. For that purpose, the normalized parameters $B_{S,q}^{nor,k}$ are first expressed in terms of the measured crystal field coefficients $B_{S,q}^k$ which only account for the spatial variation of the electric field due to the ligand(s) and are reported in the literature.[25−27] The most extensive set of tabulated data[26] are the coefficients $B_{S,q}^k$ of $H_{lig,S}$ in the basis of the tensor operators $C_q^{Wyb,k}$ chosen by Wybourne[26] (Wyb) and derived from the renormalized spherical harmonics $[4\pi/(2k + 1)]Y_{kq}(\theta,\varphi)$ of the angular position (θ, φ) of a 4f electron. The operators $C_q^{Wyb,k}$ are readily given in terms of the tensor operators T_q^k introduced by Buckmaster et al.[28] as

$$C_q^{Wyb,k} = n_k^{Wyb/Buck} T_q^k \tag{7}$$

with $n_k^{Wyb/Buck} = (3/2)^{1/2}$, $(35/8)^{1/2}$, $(231/4)^{1/2}$ for $k = 2, 4, 6$, respectively. In turn, the operators T_q^k are written in terms of the normalized operators t_q^k as

$$T_q^k = \sqrt{A_k(J)}\, t_q^k \tag{8a}$$

with

$$A_k(J) = (k!)^2 \frac{(2J + k + 1)!}{2^k(2k + 1)!(2J - k)!} \tag{8b}$$

Turn to the expressions of the Hamiltonians $H_{lig,X}$ of the static and transient ligand fields in terms of the Wybourne operators $C_q^{Wyb,k}$. Both Hamiltonians can be written as

$$H_{lig,X} = \sum_{k,q} B_{X,q}^k \langle Ln,J\|k\|Ln,J\rangle C_q^{Wyb,k} \tag{9}$$

where the reduced matrix elements $\langle Ln,J\|k\|Ln,J\rangle$ are tabulated in the form $\langle Ln,J\|k\|Ln,J\rangle = \langle J\|\alpha\|J\rangle$, $\langle J\|\beta\|J\rangle$, $\langle J\|\gamma\|J\rangle$ for $k = 2, 4, 6$, respectively (ref 25, Table 20, and Supporting Information, Table 7). Therefore, we have

$$B_{X,q}^{nor,k}/B_{X,q}^k = \langle Ln,J\|k\|Ln,J\rangle n_k^{Wyb/Buck}\sqrt{A_k(J)} \tag{10}$$

The reduced matrix elements $\langle Ln,J\|k\|Ln,J\rangle$ show complicated variations with Ln and k, with their higher values for Tm and particularly Yb. The coefficients $A_k(J)$ increase with J with a maximum for Ho along the Ln series, which is all the more pronounced as k is large. The ratios $B_{X,q}^{nor,k}/B_{X,q}^k$ reported in Table 11 reflect these dependences.

Table 11. Ratios $B_{X,q}^{nor,k}/B_{X,q}^k$ Defined by Eq 10 and Measuring the Response of the Ground J Multiplet of Ln^{3+} to the Tensorial Terms of Various Orders k of a Ligand Field

k	Tb	Dy	Ho	Er	Tm	Yb
2	−0.678	−0.72	−0.293	0.288	0.678	0.617
4	0.12	−0.304	−0.227	0.228	0.319	−0.322
6	−0.063	0.25	−0.473	0.499	−0.316	0.189

As already noted, the usual ligand field parameters $B_{X,q}^k$ only account for the spatial variation of the ligand electric field whereas their normalized counterparts $B_{X,q}^{nor,k}$, driving the electronic relaxation, describe the response of the ground J multiplet of Ln^{3+} to this field. This response results from subtle interactions between the $4f^n$ electrons involving their spin−orbit couplings and therefore depends on the Ln^{3+} ion as quantified by the ratios $B_{X,q}^{nor,k}/B_{X,q}^k$. Experimentally, the tabulated static parameters $B_{S,q}^k$ range between 100 and 1000 cm^{-1}. As expected from their purely electrostatic nature and the quite similar ionic characters of the Ln^{3+} ions, they have rather constant values along the Ln series for a given ligand field. Also, note that the terms of order 2, are often twice as small as the terms of orders 4 and 6. As discussed previously[13] and hereafter within the simple-point charge model of ligand field, the transient ligand field parameters $B_{T,q}^k$ should be of the same order of magnitude as their static counterparts, that is, $B_{T,q}^k \cong_{stat} B_{S,q}^k$, where the symbol $\cong_{stat}$ means "statistically" of the order of. Furthermore, because of their purely electrostatic nature, they should be rather constant along the Ln series for a given ligand field. Therefore, because the relative contribution of $B_{T,q}^{nor,k}t_q^k$ to $R_{le}^{Redfield}$ is simply weighted by $|B_{T,q}^{nor,k}|^2$ for a given Ln^{3+} ion, Table 11 ranks the impact of this contribution as a function of the nature of the ion. In addition, it stresses the importance of the effects of terms of order 4 and 6 on electronic relaxation, especially for Ho and Er.

Now, for a better comparison of the respective relaxation roles of the t_q^k terms among the Ln^{3+} ions, we introduce the Redfield relaxation weighting factors defined as

$$w_k^{Redfield} = 10^2(B_{X,q}^{nor,k}/B_{X,q}^k)^2/[(2J + 1)J(J + 1)] \tag{11}$$

where the factor 100 allows one to deal with values of the order of unity. These factors are reported in Table 12, emphasizing the large relaxation rates of Tm and particularly Yb, as observed.

Table 12. Redfield Weighting Relaxation Factors $w_k^{Redfield}$ Defined by Eq 11 and Ranking the Relaxation Effect of a Single Tensorial Term $B_{T,q}^{nor,k}t_q^k$ as a Function of the Ln^{3+} Ion

	Tb	Dy	Ho	Er	Tm	Yb
$w_2^{Redfield}$	8.418	5.079	0.704	0.813	8.418	30.234
$w_4^{Redfield}$	0.263	0.909	0.419	0.511	1.869	8.246
$w_6^{Redfield}$	0.073	0.611	1.829	2.443	1.826	2.846

Two additional effects contribute to the amplification of the relaxation roles of the terms of orders 4 and 6. First, the simple point-charge model[25] gives some insight into the relative magnitudes of the B_q^k parameters of the transient and static

dx.doi.org/10.1021/jp311273x | J. Phys. Chem. A 2013, 117, 905−917

ligand fields. The multipolar (mpol) electric potential V^k_{lig} of order k due to a charge at a distance R from the Ln center is given by

$$V^k_{lig}(R) \propto 1/R^{k+1} \tag{12}$$

Because of the distortions and vibrations of the complex, assume that the distance R oscillates around a mean distance R_0 by simply taking the two values $R_\pm = R_0(1 \pm \varepsilon)$. Then, the mean ligand field $\overline{V^k_{lig}}$, that is, the static ligand field, and its oscillation amplitude ΔV^k_{lig}, that is, the transient ligand field, are given by

$$\begin{cases} \overline{V^k_{lig}} \propto 0.5[V^k_{lig}(R_-) + V^k_{lig}(R_+)] \\ \Delta V^k_{lig} \propto V^k_{lig}(R_-) - \overline{V^k_{lig}} \end{cases} \tag{13}$$

Rough estimates of the transient parameters $B^k_{T,q}$ can be inferred from typical mean values $\langle B^k_{S,q} \neq 0\rangle$ of the static parameters for a given ligand, which are not canceled by symmetry. For that purpose, the transient/static ratios $B^k_{T,q}/\langle B^k_{S,q} \neq 0\rangle$ are estimated from ΔV^k_{lig} and $\overline{V^k_{lig}}$ as

$$B^k_{T,q}/\langle B^k_{S,q} \neq 0\rangle \cong_{stat} f^k_{mpol} = \Delta V^k_{lig}/\overline{V^k_{lig}} \tag{14}$$

They rise with the steepness of $V^k_{lig}(R)$, which increases with k. For instance, for a variation of ± 0.2 Å of the bonding distance $R \cong 2.5$ Å of the O and N atoms to Ln^{3+}, we have $\varepsilon \cong 0.1$ and the ratios $B^k_{T,q}/\langle B^k_{S,q} \neq 0\rangle$ are 0.29, 0.46, 0.61 for $k = 2$, 4, 6, respectively. Note that a given parameter $B^k_{T,q}$ is nearly always different from $f^k_{mpol}B^k_{S,q}$ as exemplified by the situation where the symmetry of the complex implies $B^k_{S,q} = 0$. Because the symmetry is generally not preserved by the distortions giving rise to the transient ligand field, the inequality $B^k_{T,q} \neq 0$ holds. In brief, only rough estimates of the transient parameters $B^k_{T,q}$ can be inferred from mean values of their static counterparts and there is no strict correlation between $B^k_{T,q}$ and $B^k_{S,q}$. The relative importance of the transient coefficients with respect to their static counterparts increases with k.

Second, the number of independent components of the transient ligand field is limited only by its real character, leading to the equality, $B^k_{T,q} = (-)^q B^{k*}_{T,-q}$, so that there are $k + 1$ independent terms of order k. These terms are assumed to be stochastically independent because the distortions and vibrations of the complex are fully random. Then, their effects on the relaxation add up.

The Redfield relaxation weighting factors $W^{Redfield}_k$ due to all the terms of order k of the transient ligand field are defined as

$$W^{Redfield}_k = (k + 1)(f^k_{mpol})^2 w^{Redfield}_k \tag{15}$$

They are reported in Table 13. Assuming that the mean values $\langle B^k_{S,q} \neq 0\rangle$ of the static ligand field parameters $B^k_{S,q}$ for each order k have similar sizes, these factors can be used to gauge the respective contributions of the transient terms of order k to $R^{Redfield}_{le}$.

The total weighting factor $\sum_{k=2,4,6} W^{Redfield}_k$ to $R^{Redfield}_{le}$ in Table 13 reproduces the statistical experimental sequence of the R_{le} values across the various Ln series, except for the inversion of Ho with Er, on the basis of the present crude, but reasonable, physical arguments applied to the Redfield approximation $R^{Redfield}_{le}$ due to the sole transient ligand field. Because $T^{Redfield}_{1e} \propto 1/\sum_{k=2,4,6} W^{Redfield}_k$, the contributions to the nuclear relaxation rates R_1 and R_2 of the first terms of eqs 1 and 2 are proportional to the quantities $g_{Ln}{}^2 J(J + 1)\sum_{k=2,4,6} W^{Redfield}_k$, which are reported in Table 13. The theory confirms that the complexes of Tb and Dy are among the most efficient paramagnetic enhancers of nuclear relaxation rates whereas those of Tm and Yb are the less efficient ones. Unfortunately, the Redfield approximation seems to underestimate the efficiency of Er and overestimate that of Ho. Moreover, for a transient ligand field Hamiltonian with a single fluctuating term, this approximation leads for Dy^{3+}, Ho^{3+}, and Er^{3+} to relaxation times $T_{le} \cong 0.5$ ps, often significantly longer than the measured values. Because the Redfield relaxation times are lower bounds for the actual relaxation times,[13] we have first to verify that the "exact" simulated values are sufficiently short to reproduce the experimental data. For that purpose, we consider the most demanding case of the Ho^{3+} ion, for which T_{le} has the shortest experimental values down to 0.11 ps and the longest Redfield estimate of 0.57 ps.

B. Simulation Results. The simulated values of T_{le} were defined as

$$T^{eff}_{1e} = \int_0^\infty G^{nor}_{\|}(t)\, dt$$

where $G^{nor}_{\|}(t)$ is the normalized longitudinal time correlation function (TCF) obtained by using the so-called Grenoble method, which is one of the available alternatives for computing electronic spin relaxation.[30−33] This theoretical approach is based on the numerical solution of the Schrödinger equation to obtain the evolution operator of the electronic states of the J ground multiplet of the Ln^{3+} ion as a function of the random rotational and vibrational trajectory of the complex. It employs the optimized Fortran program ERELAX discussed elsewhere in details.[33]

First, the effects of $H_{lig,S}$ on the electronic relaxation are neglected ($H_{lig,S} = 0$). In Figure 4a, the TCF $G^{nor}_{\|}(t)$ is shown for a reasonable $H_{lig,T}$ with $\|H_{lig,T}\| = 320$ cm^{-1} and a single fluctuating term. The values of T^{eff}_{le} decrease with the order of $H_{lig,T}$ as is the case for Yb^{3+} (Supporting Information, Figure 8, corrected Figure 4 of ref 13). However, they remain much too long, even for the terms of higher orders for which $G^{nor}_{\|}(t)$ is nearer to the Redfield limit because of shorter correlation times[13] $\tau_{v,4} = 0.3\tau_v$, $\tau_{v,6} = 0.14\tau_v$ ($\tau_{v,k} = 6\tau_v/[k(k + 1)]$). As shown in Figure 4b, the shortest experimental value 0.11 ps of T_{le} is not reached even for the rather high norm $\|H_{lig,T}\| = 640$ cm^{-1} with $T^{Redfield}_{1e} = 0.14$ ps and for a fast fluctuating pure cubic term of order 6.

Table 13. Redfield Weighting Relaxation Factors $W^{Redfield}_k$ Defined by Eq 15 and Ranking the Relaxation Effect Due to All the Transient Terms of Order k as a Function of the Ln^{3+} Ion

	Tb	Dy	Ho	Er	Tm	Yb
$W^{Redfield}_2$	2.16	1.30	0.18	0.21	2.16	7.75
$W^{Redfield}_4$	0.28	0.98	0.45	0.55	2.01	8.85
$W^{Redfield}_6$	0.19	1.57	4.7	6.28	4.69	7.31
$\sum_{k=2,4,6} W^{Redfield}_k$	2.63	3.85	5.33	7.04	8.86	23.91
$g_{Ln}{}^2 J(J + 1)/\sum_{k=2,4,6} W^{Redfield}_k$	0.36	0.29	0.21	0.13	0.06	0.01

dx.doi.org/10.1021/jp311273x | J. Phys. Chem. A 2013, 117, 905−917

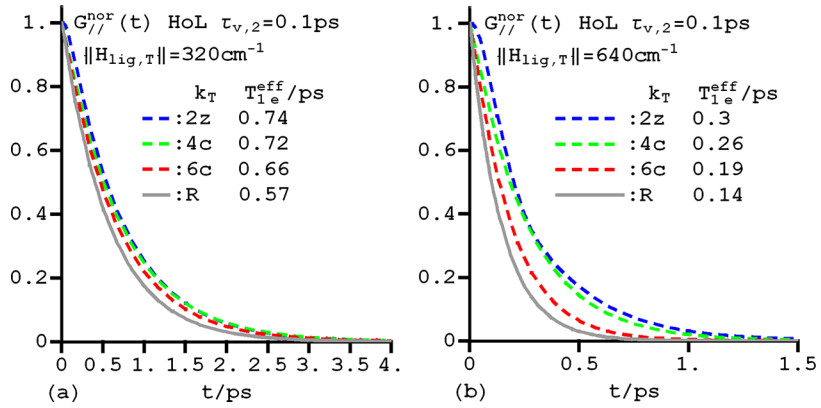

Figure 4. Time evolution of $G_{\|}^{nor}(t)$ of an HoL complex induced by various transient ligand field terms $H_{lig,T}$ of fixed magnitude $\|H_{lig,T}\|$ = 320 cm^{-1} (a) or 640 cm^{-1} (b) and vibrational correlation time $\tau_v = \tau_{v,2}$ = 0.1 ps. Notations: 2z is an axial Hamiltonian of pure order 2; 4c, 6c are cubic Hamiltonians of pure order 4 or 6; R is the result of the Redfield theory.

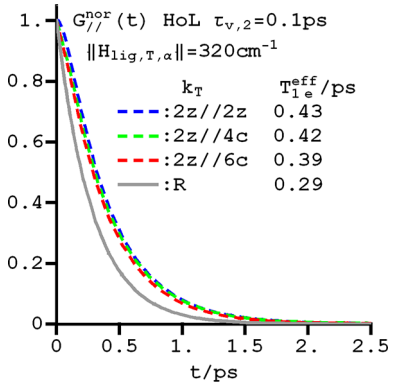

Figure 5. Time evolution of $G_{\|}^{nor}(t)$ of an HoL complex induced by various transient ligand field terms $H_{lig,T}$. Notations: the symbol $\|$ indicates the parallel action of two stochastically independent combination of tensor operators $H_{lig,T,\alpha}$ and $H_{lig,T,\beta}$ of magnitude 320 cm^{-1} and vibrational correlation time $\tau_v = \tau_{v,2}$ = 0.1 ps; α, β = 2z is an axial Hamiltonian of pure order 2; β = 4c, 6c are cubic Hamiltonians of pure order 4 or 6; R is the result of the Redfield theory.

In Figure 5 the TCF $G_{\|}^{nor}(t)$ is shown for a reasonable $H_{lig,T}$, which is the sum of two stochastically independent fluctuating terms $H_{lig,T,\alpha}$ and $H_{lig,T,\beta}$ similar to the Hamiltonians in Figure 4a. The values of T_{1e}^{eff} are nearly as short as $(T_{1e,\alpha}^{eff} T_{1e,\beta}^{eff})/(T_{1e,\alpha}^{eff} + T_{1e,\beta}^{eff})$, which demonstrates the reasonably additive character of the contributions of $H_{lig,T,\alpha}$ and $H_{lig,T,\beta}$ to the electronic relaxation rate beyond the Redfield limit because we have $\|H_{lig,T,\alpha or \beta}\|\tau_v = 6$. Then, the addition of independent fluctuating transient ligand fields is a first route toward the observed short values of T_{1e}.

In Figure 6, the modifications of $G_{\|}^{nor}(t)$ are caused by the inclusion of a static ligand field $H_{lig,S}$ of norm 320 cm^{-1} in the total ligand field Hamiltonian. The rotational correlation time τ_r of $H_{lig,S}$ is much longer than τ_v. The transient term is axial of order 2 whereas axial and cubic Hamiltonians of various pure order k_S are considered for the static term in Figure 6a–c. The values of $G_{\|}^{nor}(t)$ in the presence of the sole $H_{lig,S}$ (k_T = 0) are also plotted as references. The evolution of $G_{\|}^{nor}(t)$ due to the sole static ligand field $H_{lig,S}$ is represented by the red dotted line. Its initial decay depends only on the size of $H_{lig,S}$ and can be very fast because it is not limited by the slow fluctuations of this Hamiltonian at the picosecond time scale. Besides, these slow fluctuations do not give rise to a relaxation mechanism so that $G_{\|}^{nor}(t)$ can show marked recovery oscillations in the absence of

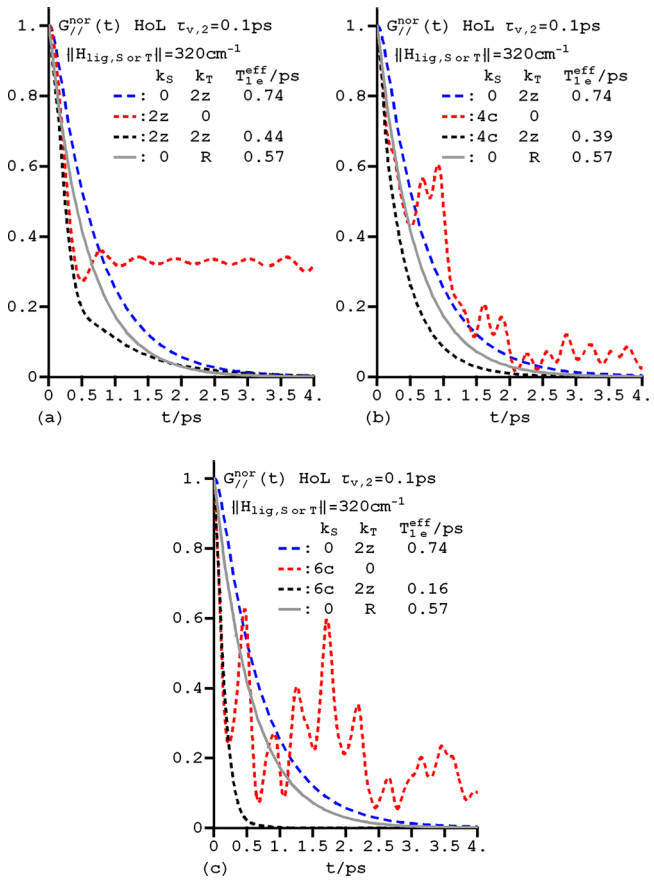

Figure 6. Time evolution of $G_{\|}^{nor}(t)$ of an HoL complex induced by an axial transient ligand field $H_{lig,T}$ of norm 320 cm^{-1} and order 2 to which is added a static ligand fields $H_{lig,S}$ of norm 320 cm^{-1} and of various orders k_S with axial or cubic symmetry. The correlation times are τ_r = 100 ps, $\tau_v = \tau_{v,2}$ = 0.1 ps. Notations: 0 indicates the absence of Hamiltonian; 2z indicates an axial term of pure order 2; 4c, 6c indicate cubic static ligand fields of pure order 4 or 6; R is the result of the Redfield theory. Effects of static terms of order 2 (a), 4 (b), 6 (c).

the transient ligand field $H_{lig,T}$. Here, $H_{lig,S}$ of large magnitude causes an initial drop of $G_{\|}^{nor}(t)$, which is significantly faster than that due to the sole transient ligand field described by the blue dashed curve and similar to that obtained by the addition of the transient ligand field and represented by the black dashed line. Then, $H_{lig,T}$ governs the continuation of the decay of $G_{\|}^{nor}(t)$.

dx.doi.org/10.1021/jp311273x | J. Phys. Chem. A 2013, 117, 905–917

Broadly speaking, $H_{lig,S}$ accelerates the initial decay of $G_{\parallel}^{nor}(t)$ giving rise to shorter relaxation times T_{le}^{eff}. The value 0.74 ps of T_{le}^{eff} due to the sole $H_{lig,T}$ decreases to 0.44, 0.39, and 0.16 ps in the presence of $H_{lig,S}$ of order 2, 4, and 6, respectively.

The efficacy of $H_{lig,S}$ for shortening T_{le}^{eff} is further illustrated in Figure 7. A transient cubic ligand field $H_{lig,T}$ of norm 480 cm^{-1}

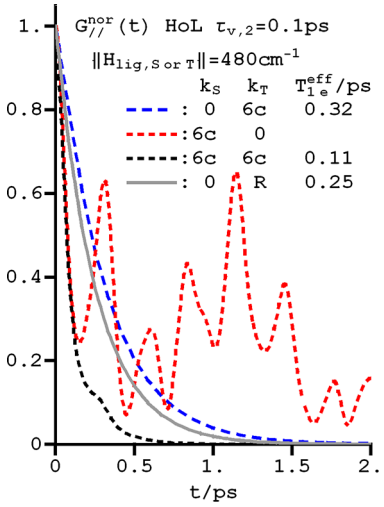

Figure 7. Time evolution of $G_{\parallel}^{nor}(t)$ of an HoL complex induced by a transient cubic ligand field $H_{lig,T}$ of norm 480 cm^{-1} and pure order $k_T = 6$ to which is added a static cubic ligand field $H_{lig,S}$ of norm 480 cm^{-1} and pure order $k_S = 6$. The correlation times are $\tau_r = 100$ ps, $\tau_v = \tau_{v,2} = 0.1$ ps. Notations: 0 indicates the absence of Hamiltonian; 6c indicates a cubic ligand field of pure order 6; R is the result of the Redfield theory.

and pure order $k_T = 6$ to which is added a static cubic ligand field $H_{lig,S}$ of norm 480 cm^{-1} and pure order $k_S = 6$ leads to $T_{le}^{eff} = 0.11$ ps, which is the shortest measured value for Ho^{3+}. The possible acceleration of electronic relaxation due to a static ligand field sheds light on the deviations of T_{le} values from their usual sequence across a given series of isostructural complexes. Indeed, because the static ligand field results from the mean geometry of the complex, its value, and therefore some of its tensorial components, can be minimal for a particular Ln^{3+} ion, leading to a lesser acceleration of electronic relaxation T_{le}. This effect is expected to be particularly noticeable in systems of high symmetry, such as the aqua, tris-DPA, and DOTP complexes, in which Tm^{3+} in the aqua and DOTP environments and Er^{3+} in the tris-DPA complex have surprisingly long T_{le} values.

A second important issue of the "exact" simulation approach is to confirm the ranking of the relative contributions of the various tensorial terms $B_{T,q}^{nor,k} t_q^k$ to the electronic relaxation rate R_{le} across the Ln series. These contributions change with the magnitude of $B_{T,q}^{nor,k}$ and the transient correlation time τ_v, contrary to what happens in the Redfield limit. Thus, we again choose a typical average value of 320 cm^{-1} for the norms of the various transient ligand field Hamiltonians and consider the two estimates 0.1 and 1 ps for τ_v. The simulated relaxation times T_{le}^{eff} due to various transient terms $H_{lig,T}$ with vibrational correlation time $\tau_v = 0.1$ ps are reported in Table 14.

As expected, the simulated times T_{le}^{eff} are just reasonably longer than their measured counterparts so that the cooperative action of a few stochastically independent transient terms or the shortening effect of a static term or both effects can easily reduce them to the measured values. A subtle effect is also observed: across the Ln series, the ratio $T_{le}^{eff,Ln}/T_{le}^{eff,Yb}$ varies to a lesser extent

Table 14. Simulated Relaxation Times, T_{le}^{eff} (ps), Due to Various Transient Terms $H_{lig,T}$ of Fixed Magnitude $\|H_{lig,T}\|$ = 320 cm^{-1} and Vibrational Correlation Time $\tau_v = 0.1$ ps[a]

	Tb	Dy	Ho	Er	Tm	Yb
2z	0.416	0.646	0.744	0.646	0.416	0.192
4c	0.363	0.619	0.722	0.619	0.363	0.085
6c	0.298	0.559	0.671	0.559	0.298	0.079

[a]Notations: 2z is an axial Hamiltonian of pure order 2; 4c, 6c are cubic Hamiltonians of pure order 4 or 6.

than its Redfield equivalent $T_{le}^{Redfield,Yb}/T_{le}^{Redfield,Yb}$ of Table 10. The effect is particularly important for $H_{lig,T}$ of order 2. For instance, $T_{le}^{eff,Ho}/T_{le}^{eff,Yb}$ is more than 2 times smaller than the Redfield value.

This effect is best appreciated by considering the ratios $R_{le}^{eff}/R_{le}^{Redfield}$ of the simulated and Redfield electronic relaxation rates. These ratios, given in Table 15, demonstrate that the Redfield

Table 15. Ratios $R_{le}^{eff}/R_{le}^{Redfield}$ of the Simulated and Redfield Relaxation Rates Due to Various Transient Terms $H_{lig,T}$ of Fixed Magnitude $\|H_{lig,T}\|$ = 320 cm^{-1} and Vibrational Correlation Time $\tau_v = 0.1$ ps[a]

	Tb	Dy	Ho	Er	Tm	Yb
2z	0.61	0.74	0.766	0.74	0.61	0.31
4c	0.7	0.768	0.79	0.768	0.7	0.689
6c	0.852	0.851	0.851	0.851	0.852	0.743

[a]Notations: 2z is an axial Hamiltonian of pure order 2; 4c, 6c are cubic Hamiltonians of pure order 4 or 6.

limit is all the more accurate as the angular momentum, J, is larger or the tensorial order, k, is higher. Indeed, as J increases, T_{le} becomes progressively much longer than the transient correlation times $\tau_{v,k}$, making the Redfield approximation more and more accurate. Moreover, this property is all the better satisfied as $\tau_{v,k}$ is short, that is, k is high.

The simulated relaxation times T_{le}^{eff} and the ratios $R_{le}^{eff}/R_{le}^{Redfield}$ due to various transient terms $H_{lig,T}$ of fixed magnitude $\|H_{lig,T}\|$ = 320 cm^{-1} and longer vibrational correlation time[34] $\tau_v = 1$ ps are reported in the Supporting Information, Tables 8 and 9, respectively. For $k = 2$ and Yb, the times T_{le} with $\tau_v = 1$ ps are somewhat longer than their equivalents with $\tau_v = 0.1$ ps, but the reverse is true in all other situations. The long value of $\tau_v = \tau_{v,2}$ drastically limits the shortening of T_{le}^{eff} toward the unreasonably short Redfield limit, when the electronic relaxation is driven by a transient ligand field of order 2. In contrast, the limitation becomes less severe as the order k of the ligand field increases because $\tau_{v,4} = 0.3$ ps and $\tau_{v,6} = 0.14$ ps are much shorter than τ_v. Then, the variation of the ratio $T_{le}^{eff,Ln}/T_{le}^{eff,Yb}$ across the Ln series is further reduced. For instance, for the transient terms of order 2 and 6, $T_{le}^{eff,Ho}/T_{le}^{eff,Yb}$ is more than 5 times smaller than the Redfield value $T_{le}^{Redfield,Ho}/T_{le}^{Redfield,Yb}$ in Table 10.

Because τ_v sets lower bounds to T_{le}, the simulated T_{le}^{eff} values of the Supporting Information, Table 8 are a little different from those of Table 14, whereas the Redfield theory predicts a 10 times shortening due to a 10-fold increase of τ_v. The rather modest variation of T_{le}^{eff} with τ_v is one of the key findings explaining the small observed changes of T_{le}. Furthermore, the variation of the ratio T_{le}^{Ln}/T_{le}^{Yb} across the Ln series is smaller for the simulations than in the Redfield limit and is in better agreement with experiment.

Finally, refined relaxation factors W_k accounting for the simulation results can be deduced from their Redfield counterparts

dx.doi.org/10.1021/jp311273x | J. Phys. Chem. A 2013, 117, 905−917

$W_k^{Redfield}$ defined by eq 15 and reported in Table 13 though simple scaling by the factors $(R_{1e}^{eff}/R_{1e}^{Redfield})(k)$ of Table 15 and Supporting Information, Table 9. Then, the contributions to the nuclear relaxation rates R_1 and R_2 of the first terms of eqs 1 and 2 are proportional to the quantities $g_{Ln}^2 J(J+1)/\sum_{k=2,4,6} W_k$. Again, the statistical experimental sequence of the R_{1e} values across the various Ln series is reproduced, except for the inversion of Ho with Er. The origin of this discrepancy is caused by a weakness of the theory or by a possible statistical bias toward long T_{1e} for Er, given that the number of studied isostructural series is still small. The complexes of Tb and Dy are among the most efficient paramagnetic enhancers of nuclear relaxation rates, whereas those of Tm and Yb are among the least efficient.

6. CONCLUSIONS AND PERSPECTIVES

Analysis of the field dependence of nuclear relaxation rate data using global minimization methods allows self-consistent estimates to be made of electronic relaxation times, T_{1e}, for the fast-relaxing Ln(III) ions, in four isostructural sets of coordination complexes. Values of T_{1e} fall in the range 0.1−0.63 ps, suggesting that a physical model based on fluctuations in the transient ligand field arising from solvent−ligand collisions is reasonable. The electronic relaxation times obtained were found to be independent of solvent viscosity and applied magnetic field, and followed a common sequence: [Dy, Tb, Er] > Ho > [Tm, Yb]. The surprisingly low value of T_{1e} for Ho complexes, suggests that these complexes are less good choices as MR relaxation probes than might have been surmised earlier on the basis of its high μ_{eff} value, especially at low magnetic fields.

The order of the experimental T_{1e} values seemed to follow the sequence of second-order static ligand field coefficients, $B_{S,0}^2$, the impact of which on electronic relaxation had to be clarified. Accordingly, the weakness of the correlation between the values of the transient ligand field coefficients $B_{T,q}^k$ and their static counterparts $B_{S,q}^k$ for a given complex has been pointed out, especially in situations of static symmetry. Furthermore, the theoretical model based on the creation of a transient ligand field induced by solvent collision has been refined to account for the effect that the second and higher order parameters, $B_{T,q}^k$ and $B_{S,q}^k$, of the transient and static ligand fields may have in defining T_{1e}. Their sign and magnitude may vary considerably from one ligand field to another, and their relative weighting is shown to be sensitive to the nature of the lanthanide ion. The refined theory accommodates the available data well and highlights the importance of higher order ligand field terms (especially those of order 6) in determining the rate of electronic relaxation. This effect is particularly evident for holmium complexes.

To go beyond the statistical analysis presented here, the transient and static ligand fields should be accurately determined for each investigated Ln^{3+} ion. This is a prerequisite to a valuable interpretation of the T_{1e} sequence for the complexes $Ln.L^1$ to $Ln.L^4$. An interesting approach, developed recently, involves ab initio molecular dynamics of complexed Ln^{3+} ions, because this method easily and accurately operates at the picosecond time scale of the fluctuations of the transient ligand field.[41] Furthermore, it has been shown that the relaxation of the total electronic angular momentum of ground magnetic multiplets of high dimensions, such as that of holmium, can now be computed, making it possible to explore the electronic relaxation of the many systems with several coupled spins,[42] beyond the Redfield limit.[30−34]

■ ASSOCIATED CONTENT

Supporting Information

Tables of measured ^{1}H relaxation rates and corresponding calculated values for the internuclear distance, the rotational correlation time, and the electronic relaxation time. Table of measured ^{19}F and ^{1}H relaxation rates. Figures of ^{1}H and ^{19}F R_1 vs magnetic field. Figures of simulation of the dependence of the ^{1}H, ^{19}F, and ^{31}P relaxation rate on the electronic relaxation rate. Tables of ground state properties, simulated relaxation times, and $R_{1e}^{eff}/R_{1e}^{Redfield}$ ratios. This material is available free of charge via the Internet at http://pubs.acs.org.

■ AUTHOR INFORMATION

Corresponding Author

*E-mail: D.P., david.parker@durham.ac.uk; P.H.F., pascal-h.fries@cea.fr.

Notes

The authors declare no competing financial interest.

■ ACKNOWLEDGMENTS

We thank the EPSRC and the ERC for support (to DP: FCC 266084), and Dr. Ilya Kuprov (Southampton University) for earlier guidance and invaluable advice. This work is dedicated to Silvio Aime, a master of the magnetic resonance experiment and its application to imaging.

■ REFERENCES

(1) (a) Di Pieto, S.; Lo Piano, S.; Di Bari, L. *Coord. Chem. Rev.* **2011**, *255*, 2810. (b) Terazzi, E.; Rivera, J. P.; Ouali, N.; Piguet, C. *Magn. Reson. Chem.* **2006**, *44*, 539. (c) Peters, J. A.; Huskens, J.; Raber, D. J. *Nucl. Magn. Reson. Spectrosc.* **1996**, *28*, 282.

(2) (a) Balogh, E.; Wu, D.; Zhou, G.; Gochin, M. *J. Am. Chem. Soc.* **2009**, *131*, 2821. (b) Bertini, I.; Del Bianco, C.; Gelis, I.; Katsaros, N.; Luchinat, C.; Parigi, G.; Peana, M.; Provenzani, A.; Zoroddu, M. A. *Proc. Natl. Acad. Sci. U. S. A.* **2004**, *101*, 6841.

(3) Fries, P. H. *J. Chem. Phys.* **2012**, *136*, 044504.

(4) (a) Pintacuda, G.; John, M.; Su, X.-C.; Otting, G. *Acc. Chem. Res.* **2007**, *40*, 206. (b) Otting, G. *J. Biomol. NMR* **2008**, *42*, 1.

(5) (a) Harvey, P.; Kuprov, I.; Parker, D. *Eur. J. Inorg. Chem.* **2012**, 2015. (b) Chalmers, K. H.; De Luca, E.; Hogg, N. H. M.; Kenwright, A. M.; Kuprov, I.; Parker, D.; Botta, M.; Wilson, J. I.; Blamire, A. M. *Chem.—Eur. J.* **2010**, *16*, 134. (c) Aime, S.; Botta, M.; Parker, D.; Williams, J. A. G. *J. Chem. Soc., Dalton Trans.* **1995**, 2259.

(6) (a) Goldman, M. *J. Magn. Reson.* **2001**, *149*, 160. (b) Gueron, M. *J. Magn. Reson.* **1995**, *19*, 58.

(7) (a) Bertini, I.; Luchinat, C.; Parigi, G. *Solution NMR of Paramagnetic Molecules*; Elsevier: Amsterdam, 2001. (b) Gignoux, D.; Schmitt, D.; Zeguine, M. *J. Magn. Magn. Mater.* **1987**, *66*, 373. (c) Chevalier, B.; Tence, S.; Andre, G.; Matier, S. F.; Gueden, E. *J. Phys. Conf. Ser.* **2010**, 032012.

(8) Vigouroux, C.; Belorizky, E.; Fries, P. H. *Eur. Phys. J. D* **1999**, *5*, 243.

(9) Aime, S.; Borboo, L.; Botta, M.; Ermondi, G. *J. Chem. Soc., Dalton Trans.* **1992**, 225.

(10) Ren, J. M.; Sherry, A. D. *J. Magn. Reson. Ser. B.* **1996**, *111*, 178.

(11) (a) Alsaadi, B. M.; Rossotti, F. J. C.; Williams, R. J. P. *J. Chem. Soc., Dalton Trans.* **1980**, 2147. (b) Alsaadi, B. M.; Rossotti, F. J. C.; Williams, R. J. P. *J. Chem. Soc., Dalton Trans.* **1980**, 2151.

(12) Bertini, I.; Capozzi, F.; Luchinat, C.; Nicastro, G.; Xie, G. C. *J. Phys. Chem.* **1993**, *97*, 6351.

(13) Fries, P. H.; Belorizky, E. *J. Chem. Phys.* **2012**, *136*, 074513.

(14) Hopkins, T. A.; Bolender, J. P.; Metcalf, D. H.; Richardson, F. S. *Inorg. Chem.* **1996**, *35*, 5347.

(15) (a) Kang, J.-G.; Na, M.-K.; Yoon, S.-K.; Sohn, Y.; Kim, Y.-D.; Suh, I.-H. *Inorg. Chim. Acta* **2000**, *310*, 56. (b) Kang, J.-G.; Kim, T.-J. *Bull. Korean Chem. Soc.* **2005**, *26*, 1057.

(16) (a) Walton, J. W.; Di Bari, L.; Parker, D.; Pescitelli, G.; Puschmann, H.; Yufit, D. S. *Chem. Commun.* **2011**, *47*, 12289. (b) Walton, J. W.; Carr, R.; Evans, N. H.; Funk, A. M.; Kenwright, A. M.; Parker, D.; Yufit, D. S.; Botta, M.; De Pinto, S.; Wang, K.-L. *Inorg. Chem.* **2012**, *51*, 8042.
(17) (a) Gateau, C.; Mazzanti, M.; Pecant, F.; Dunand, F.; Helm, C. *Dalton Trans.* **2003**, 2428. (b) Nocton, G.; Nonat, A.; Gateau, C.; Mazzanti, M. *Helv. Chim. Acta* **2009**, *92*, 2257.
(18) Parker, D.; Puschmann, H.; Batsanov, A. S.; Senanyake, K. *Inorg. Chem.* **2003**, *42*, 8646.
(19) Schmid, F.; Holtke, C.; Parker, D.; Faber, C. *Magn. Reson. Med.* **2012**, *67*, in press.
(20) (a) Chalmers, K. H.; Kenwright, A. M.; Parker, D.; Blamire, A. M. *Magn. Reson. Med.* **2011**, *66*, 931. (b) Chalmers, K. H.; Botta, M.; Parker, D. *Dalton Trans.* **2011**, *40*, 904.
(21) Holz, M.; Mao, X. A.; Seiferling, D.; Sacco, A. *J. Chem. Phys.* **1996**, *104*, 669.
(22) (a) Binnemans, K.; Gorlier-Walrand, C. *Chem. Phys. Lett.* **1995**, *245*, 75. (b) Gorlier-Walrand, C.; Huygen, E.; Binnemans, K.; Fluyt, L. *J. Phys.: Condens. Matter* **1994**, *6*, 7797.
(23) Bleaney, B. *J. Magn. Reson.* **1972**, *8*, 91.
(24) Dickins, R. S.; Parker, D.; Bruce, J. I.; Tozer, D. J. *Dalton Trans.* **2003**, 1264.
(25) Abragam, A.; Bleaney, B. *Résonance Paramagnétique Electronique des Ions de Transition*; Presses Universitaires de France: Paris, 1971.
(26) Morrison, C. A.; Leavitt, R. P. Spectroscopic Properties of triply ionized lanthanides in transparent host crystals. In *Handbook on the Physics and Chemistry of Rare Earths*; Geschneider, K. A., Eyring, L., Eds.; North-Holland: Amsterdam, 1982; Vol. 5, pp 461−692.
(27) Ishikawa, N. *J. Phys. Chem. A* **2003**, *107*, 5831−5835.
(28) Buckmaster, H. A.; Chatterjee, R.; Shing, Y. H. *Physica Status Solidi A* **1972**, *13*, 9−49.
(29) Blum, K. *Density Matrix Theory and Applications*; Plenum Press: New York, 1981.
(30) Kowalewski, J.; Kruk, D.; Parigi, G. *Adv. Inorg. Chem.* **2005**, *57*, 41.
(31) Belorizky, E.; Fries, P. H.; Helm, L.; Kowalewski, J.; Kruk, D.; Sharp, R. R.; Westlund, P.-O. *J. Chem. Phys.* **2008**, *128*, 052315.
(32) Aman, K.; Westlund, P. O. *Phys. Chem. Chem. Phys.* **2007**, *9*, 691.
(33) Fries, P. H.; Belorizky, E. *J. Chem. Phys.* **2007**, *126*, 204503.
(34) Fries, P. H. *Eur. J. Inorg. Chem.* **2012**, 2156−2166.
(35) Caravan, P.; Ellison, J. J.; McMurry, T. J.; Lauffer, R. B. *Chem. Rev.* **1999**, *99*, 2293.
(36) Powell, D. H.; NiDhubhghaill, O. M.; Pubanz, D.; Helm, L.; Lebedev, Y. S.; Schlaepfer, W.; Merbach, A. E. *J. Am. Chem. Soc.* **1996**, *118*, 9333.
(37) Rast, S.; Fries, P. H.; Belorizky, E. *J. Chim. Phys. Phys.-Chim. Biol.* **1999**, *96*, 1543.
(38) Rast, S.; Borel, A.; Helm, L.; Belorizky, E.; Fries, P. H.; Merbach, A. E. *J. Am. Chem. Soc.* **2001**, *123*, 2637.
(39) Bonnet, C. S.; Fries, P. H.; Gadelle, A.; Gambarelli, S.; Delangle, P. *J. Am. Chem. Soc.* **2008**, *130*, 10401.
(40) Lindgren, M.; Laaksonen, A.; Westlund, P. O. *Phys. Chem. Chem. Phys.* **2009**, *11*, 10368.
(41) Pollet, R.; Nair, N. N.; Marx, D. *Inorg. Chem.* **2011**, *50*, 4791.
(42) Belorizky, E.; Fries, P. H. *J. Chim. Phys. Phys.-Chim. Biol.* **1993**, *90*, 1077.